Magnetic nanoparticles as components of magnetoresistance sensors: the gGMR-sensor

A. Weddemann*, M. Zahn*, I. Ennen**, A. Regtmeier***, and A. Hütten***

* Massachusetts Institute of Technology, RLE, MA, USA, weddeman@mit.edu
** Vienna University of Technology, Institute of Solid State Physics, Vienna, Austria
*** Bielefeld University, Department of Physics, Bielefeld, Germany

ABSTRACT

The granular giant magnetoresistance effect is employed for the conceptional design of a novel type of magnetoresistive sensor. By solving the Landau-Lifshitz equation for a set of homogeneously magnetized spheres arranged in an ordered monolayer of cubic or hexagonal symmetry, we found the absence of exchange coupling between spatially separated magnetic material to result in the antiparallel alignment of contiguous magnetic nanoparticles. The switching behaviour of these arrays is soft in comparison to continuous sensors and the influence of the component properties on the response functions indicate constructive methods to tailor the sensor characteristics to specific needs by the employment of selected particles. Further, we will show that in the case of low distance measurements, an increased sensitivity, in comparison to the conventional magnetoresistance sensors, is bought at the cost of an inherent device noise.

Keywords: magnetic nanoparticles, monolayers, granular giant magnetoresistance, magnetoresistive sensor

1 INTRODUCTION

Superparamagnetic beads and nanoparticles have a wide range of applications in the field of microfluidic lab-on-a-chip devices [1]. In an external magnetic field, they align their magnetic moments parallel to the field direction. This allows not only for their manipulation by inhomogeneous magnetic fields but also gives rise to a dipolar stray field. These stray fields themselves influence soft magnetic material nearby which allows for the magnetic recognition of such particles by magnetoresistive (MR) sensors [2]–[4]. Such sensors consist of various layers with a soft ferromagnetic top electrode which acts as a sensing element.

Downscaling these devices results in a high magnetic stiffness and sensor elements are no longer sensitive to small field variations which is one of the major challenges when designing MR sensors below the micron size [5], [6]. By the employment of assemblies of superparamagnetic particles, the magnetic confinement is broken by spatial separation. Each particle in such an arrangement forms its own magnetic domain which couples to contiguous particles via its stray field entailing a magnetic superstructure of antiferromagnetic domains. Due to spin-dependent transport phenomena, such a particle sheet may serve as a *granular giant magnetoresistance* (gGMR) sensor capable of detecting and monitoring other magnetic sources.

2 FERROMAGNETIC SYSTEMS

Magnetoresistive sensors and magnetic nanoparticles consist of ferromagnetic materials, i.e., at every point of the magnetic volume, the magnetization vector $\mathbf{M} = M_\mathrm{S}\hat{\mathbf{m}}$ is of a constant absolute value, the material dependent *saturation magnetization* M_S. Therefore, the macroscopic properties of the object result from the orientation $\hat{\mathbf{m}}$. Starting from a given initial configuration, the dynamic evolution of the system is governed by the empirical *Landau-Lifshitz*-equation [7]

$$\frac{\partial\hat{\mathbf{m}}}{\partial t} - \alpha\hat{\mathbf{m}}\times\frac{\partial\hat{\mathbf{m}}}{\partial t} = \gamma\hat{\mathbf{m}}\times\mathbf{H}_\mathrm{eff}, \tag{1}$$

with α a dimensionless parameter summarizing all local microscopic damping phenomena and γ the gyromagnetic ratio. The effective magnetic field $\mathbf{H}_\mathrm{eff}$ resembles all field-like contributions that result in a torque density $\mathbf{M}\times\mathbf{H}$ acting on the magnetization. Various contributions are usually taken into account:

$$\mathbf{H}_\mathrm{eff} = \frac{2A}{\mu_0 M_\mathrm{S}}\Delta\hat{\mathbf{m}} - \frac{\delta f_\mathrm{ani}(\hat{\mathbf{m}})}{\delta\hat{\mathbf{m}}} + \mathbf{H}_\mathrm{demag} + \mathbf{H}_\mathrm{ext} \tag{2}$$

with the exchange constant A and anisotropy functional f_ani. The individual terms represent the microscopic exchange coupling, the magnetocrystalline anisotropy influence due to spin-orbit coupling, the demagnetization field $\mathbf{H}_\mathrm{demag}$ and external field contributions $\mathbf{H}_\mathrm{ext}$, respectively.

Equations 1 and 2 describe the behaviour of all macroscopic ferromagnetic objects, so how do magnetic film and nanoparticle systems differ from each other? The reason can be found in the exchange coupling which may be understood as a resistance against spatial variations of the magnetization direction; ferromagnetic objects tend to align contiguous atomic spins parallel to each other. In case of a thin magnetic layers with a thickness of only several nanometers, the exchange energy

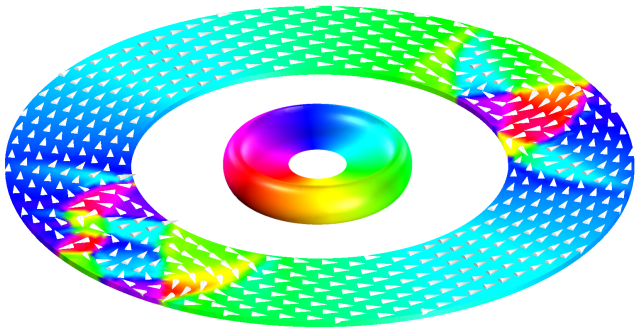

Figure 1: Magnetization distribution of a thin magnetic ring film of 10 nm thickness. Inner and outer radius are chosen 300 and 500 nm, respectively, magnetic parameters are set to $M_S = 1000$ kA/m and $A = 10^{-12}$ J/m. The inner circle represents the color scale of the distribution of magnetization direction.

does not allow for a change of orientation perpendicular to the film plane. Therefore, the magnetization vector may be written as $\mathbf{M}(\mathbf{r}) = \mathbf{M}(x, y)$. Figure 1 shows the magnetic state of a thin ferromagnetic ring under the assumption of an isotropic crystal structure, $f_{\text{ani}} \equiv 0$. The circular color code represents the magnetic orientation of the in-plane components.

2.1 Magnetic nanoparticles

Due to the dimensions of magnetic nanoparticles such a relation holds for all three space directions and, consequently, the magnetization is a constant along the magnetic volume. For a constant distribution, the curvatures of the components m_i vanish and equations 1, 2 simplify from a system of partial differential equations to a set of ordinary ones [8]. Considering N such particles, the set of equations can be rewritten in matrix form as

$$(\mathsf{Id} - \alpha\mathsf{M})\frac{\partial \mathsf{m}}{\partial t} = \gamma \mathsf{M}\mathsf{H}_{\text{eff}} \tag{3}$$

with Id the identity mapping on $\mathbb{R}^{3N\times 3N}$, by M the block diagonal matrix

$$\mathsf{M} = \begin{pmatrix} \mathsf{M}_1 & & 0 \\ & \ddots & \\ 0 & & \mathsf{M}_N \end{pmatrix}$$

with $\mathsf{M}_{n,ij} = \epsilon_{ijk}\hat{m}_{n,k}, n = 1, ..., N$ and

$$\frac{\partial \mathsf{m}}{\partial t} = \frac{\partial}{\partial t}(\hat{m}_{x,1}, \hat{m}_{y,1}, ..., \hat{m}_{x,2}, ...)^T$$
$$\mathsf{H}_{\text{eff}} = (H_{\text{eff},x,1}, H_{\text{eff},y,1}, ..., H_{\text{eff},x,2}, ...)^T.$$

The external magnetic stray field of the particles can be approximated by a dipole expression due to their homogeneous magnetization distribution [9]. In particular,

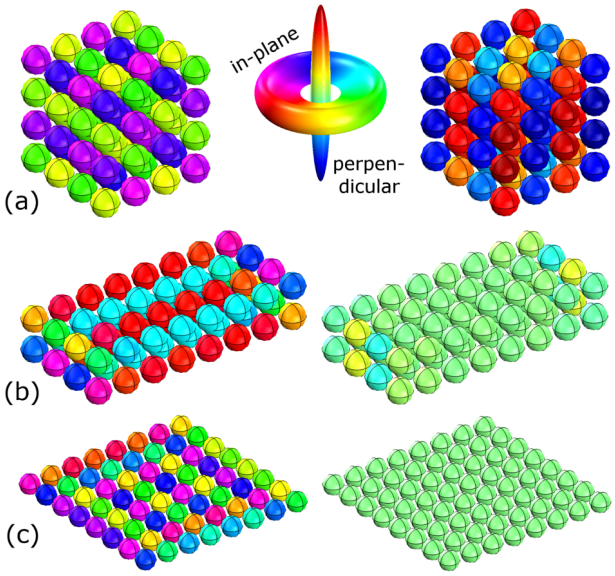

Figure 2: Equilibrium states of various magnetic particle assemblies. Particles with diameter of $d = 16$ nm and a saturation magnetization of $M_S = 1000$ kA/m are employed. The left side shows the xy-magnetization, the right the z-component.

the effective magnetic field reduces to anisotropy contributions and the external magnetic field which is given by the summation of particle field of magnetic nanoparticles nearby and an additional homogeneous contribution described in the following.

2.2 Magnetic equilibrium states

The absence of the exchange coupling contribution has a strong impact on the resulting magnetic patterns. Figure 2 shows examples of magnetic equilibrium states of 64 particles of diameter $d = 8$ nm of magnetization $M_S = 1000$ kA/m that are arranged along a cubic grid of lattice parameter $a = 10$ nm in the configurations (a) $4 \times 4 \times 4$, (b) $8 \times 4 \times 2$ and (c) $8 \times 8 \times 1$. Starting from a random initial state, equation 3 is integrated with respect to time. In order to provide fast convergence, the damping parameter was set to $\alpha = 1$ [10]. The left side of Figure 2 shows the angular component of the projection of the magnetic vector to the xy-plane (colorcode: disc) and the right side the component m_z (colorcode: inner cone). Without exchange coupling, the minimization of the external energy becomes the main driving force of the system. A configuration of contiguous magnetic moments into closed loops is entailed. In particular, the total magnetization of the ensemble is approximately 0. During the transition (a) $\rightarrow$ (c) from a three-dimensional to a two-dimensional particle assembly, the individual magnetic moments align perpendicular to the z-direction, similar to the situation of magnetic films (Figure 1). In contrast to the continuous

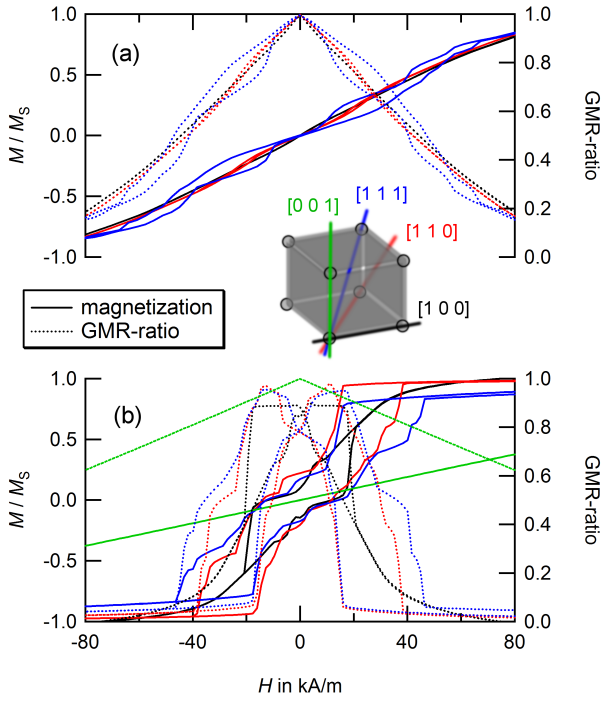

Figure 3: Response of magnetic particle ensembles to an external magnetic field for (a) $4\times4\times4$ and (b) $8\times8\times1$. Calculations are carried out along indicated directions

thin film, which shows a smooth magnetization distribution along vast areas, monolayers of nanoparticles enter a state of maximum curvature in the sense that small magnetization loops are formed.

2.3 Giant magnetoresistance effects

The GMR-effect (Nobel prize, 2007) was originally found and studied in magnetic multilayer systems [11], [12]. The resistance of a magnetic thin film device varies strongly depending on the relative orientatation of the magnetization within the layers and, therefore, can be manipulated by an external magnetic field. In 1992, Berkowitz et al. [13] and, independently, Xiao et al. [14] reported similar observations within granular systems of magnetic particles encapsulated in a metallic matrix. The GMR-ratio of such discrete magnetic patterns is correlated to the deviations of angular distribution from the average direction. According to V. Wiser [15], it is

$$\mathrm{GMR} = 1 - \frac{C}{2}\langle 1+\cos\theta\rangle^2, \qquad (4)$$

where C is a measure for the spin dependence of electron scattering and θ the angle between adjacent magnetic moments. For the sake of simplicity, we will set $C = 1$ in the following.

3 THE gGMR-SENSOR

In order to design an MR-sensor, the nanoscale system needs to meet two basic requirements [16]: (a) the susceptibility should be high in order to provide a high sensitivity and (b) the GMR-value along the measurement range needs to be biuniquely correlated to the applied field. Figure 3 shows the response functions for (a) the assembly $4\times4\times4$ and (b) $8\times8\times1$. Calculations are carried out along the indicated symmetry axes. In comparison to the three dimensional assembly, the two-dimensional monolayer meets the above mentioned requirements to a higher extent: the susceptibility of the two-dimensional array for measurements along in-plane fields is significantly higher since magnetic saturation is reached at a lower magnetic field value. The spatial confinement in the xy-plane entails a non-zero in-plane coercive field $H_{c,\parallel}$ and a paramagnetic response of low susceptibility for out-of-plane measurements. The hysteretic response results in two different GMR-H-curves which are symmetric to $H = 0$ and show monotonic slopes between the maximum and the minimum GMR-ratio. The existence of this area forms the conceptional basis for the employment as a magnetic field sensor: the monotonic behavior allows for a biunique mapping relation between the applied field and the measured GMR-value.

3.1 Influence of properties

With a wide range of different magnetic nanoparticles already available, it is interesting to understand to what extent the magnetic properties of such assemblies may be adjusted to specific needs by the modification of the nanocomponents. Due to their higher practical relevance, we will consider a 10×10-hexagonally ordered monolayer of 16 nm particles in the following. Figure 4 shows the calculated response functions for different magnetization and anisotropy assumptions, as indicated. For the case of uniaxial and cubic anisotropies, we assume that the anisotropy orientations vary independently from one particle to another.

The results show a variety of possibilities: a modification of the coupling strength (M_S) allows for the broadening of the plateaus around the GMR-maxima, while the introduction of magnetocrystalline anisotropy results in a shift of their positions. A more detailed analysis will be part of future work.

3.2 Spatial resolution

In order to analyze the capability of the particle array to determine the position of a magnetic object, we bring a magnetic probe particle of radius R_P and magnetization $\mathbf{M} = M_P\hat{\mathbf{z}}$ close to the sensor. According to the results presented in Figure 3, the setup exhibits paramagnetic behaviour with a susceptibility $\chi_\perp \ll \chi_\parallel$.

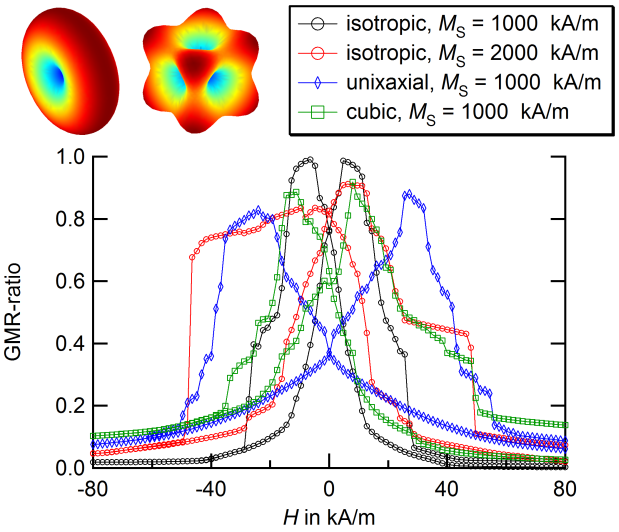

Figure 4: Response to magnetic field for different various properties of the magnetic components. The surfaces in the upper left represent the angular energy dependency for uniaxial (left) and cubic (right) symmetries where blue and red correspond to energy minima and maxima, respectively.

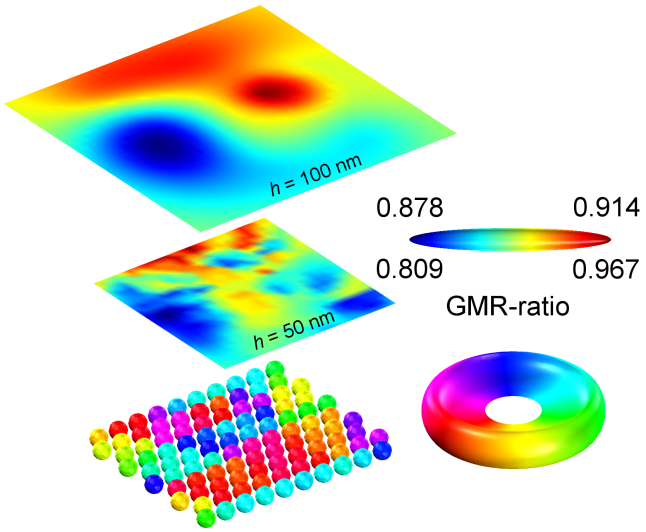

Figure 5: Magnetic response in respect to the position of probe particle of radius $R_P = 20$ nm, magnetization $M_P = 1000$ kA/m and height $z_0 = 50$ and 100 nm.

Therefore, we may neglect the external field necessary, to align the magnetization of the probe particle. In order to calculate the response of the sensor to the probe particle in respect to its coordinates, we introduce a discrete position mesh x_i, y_j, z_0 and place the probe particle at one of the nodes at a time and solve equation 3. The results are presented in Figure 5.

At some distance, we obtain a smooth response map. The magnetic field of the particle induces small deviations from the magnetic equilibrium state and the response resembles the in-plane component of the particle field itself. However, at close distances, the particle stray field overcomes the interparticle coupling. This results in a significantly higher response but is superimposed by an inherent noise signal which originates from the geometrical substructure of the device.

4 CONCLUSION

By solving the Landau-Lifshitz equation, we have studied monolayers of magnetic nanoparticles as a granular magnetoresistance sensor. We found that, in contrast to three-dimensional assemblies, applied magnetic field and GMR-ratio are biuniquely connected due to the two-dimensional spatial distribution and the entailed magnetic in-plane confinement. A smooth switching characteristic of the magnetic state was found which allows for the employability of such assemblies as magnetic field sensors. We were able to report first indications that the properties of the nanocomponents themselves may be readily modified to design a spintronic device tailored to a specific measurement task. A thorough analysis will be part of future work.

We also found that a gGMR-sensor has two working regimes. In the case of weak magnetic probes, the operational mode is similar to a conventional magnetoresistive sensor. Once the measured field exceeds a critical threshold, an increased sensitivity is achieved which is bought at the cost of inherent device noise originating from the geometrical substructure of the assembly.

REFERENCES

[1] N. Pamme, Lab Chip, 6, 24-38, 2006.
[2] S.X. Wang, G. Li, IEEE Trans. Magn., 44, 1687-1702, 2008.
[3] W. Schepper et al., J. Biotechnol., 112, 35-46, 2004.
[4] A. Weddemann et al., Biosens. Bioelec., 26, 1152-1163, 2010.
[5] C. Albon et al., APL, 95, 023101, 2009.
[6] C. Albon et al., APL, 95, 163106, 2009.
[7] L.D. Landau, E. Lifshitz, Phys. Z. Sowjetunion, 8, 153-169, 1935.
[8] D. Laroze et al., JMMM, 320, 1440-1448, 2009.
[9] J.D. Jackson in: Classical Electrodynamics, 2nd ed., Wiley, New York, 1975.
[10] A. Weddemann et al., JMMM, 322, 643-646, 2010.
[11] P. Grünberg et al., PRL, 57, 2442, 1986.
[12] M.N. Baibich et al., PRL, 61, 2472, 1988.
[13] A.E. Berkowitz et al., PRL, 68, 3745-3748, 1992.
[14] J.Q. Xiao, S. Jiang, C.L.Chien, PRL, 68, 3749-3752, 1992.
[15] N. Wiser, JMMM, 159, 119-124, 1996.
[16] A. Weddemann et al., Beilstein J. Nanotech., 1, 75-93, 2010.